ACS APPLIED MATERIALS & INTERFACES

Research Article

www.acsami.org

One-Step Synthesis of Stoichiometric $Cu_2ZnSnSe_4$ as Counter Electrode for Dye-Sensitized Solar Cells

Yan-Fang Du, Jun-Qi Fan, Wen-Hui Zhou, Zheng-Ji Zhou, Jie Jiao, and Si-Xin Wu*

The Key Laboratory for Special Functional Materials of MOE, Henan University, Kaifeng 475004, China

Supporting Information

ABSTRACT: $Cu_2ZnSnSe_4$ (CZTSe) nanoparticles with diameters of 200−300 nm were synthesized by one-step solvothermal method without surfactants or templates. The structure, composition and morphology of CZTSe nanoparticles were characterized by XRD, XPS, Raman spectrum, EDS, FESEM and TEM. The results indicated that the nanoparticles were single phase and nearly stoichiometric composition. CZTSe nanoparticles drop-casted onto FTO substrate were used as counter electrode (CE) in dye-sensitized solar cells (DSSCs) for the first time, which exhibited Pt-like electrocatalytic activity for the reduction of I_3^- to I^- in DSSCs. The *J*−*V* results demonstrated that the thickness of the film affected the photocurrent density and fill factor remarkably, which resulted from the difference of electrocatalytic sites and resistance with different thickness films. And a best efficiency of 3.85% was obtained by adjusting the film thickness. The work presents a new approach for developing low-cost, facile fabrication CZTSe nanoparticles, and demonstrates CZTSe can be explored as a low-cost alternative for expensive and scare Pt in DSSCs.

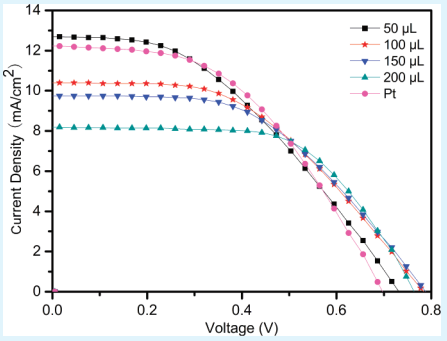

KEYWORDS: *$Cu_2ZnSnSe_4$, nanoparticles, solvothermal, counter electrode, dye-sensitized solar cells*

1. INTRODUCTION

Dye-sensitized solar cells (DSSCs) have become a "top runner" among third-generation solar cells[1] because of the advantages of low cost, environmental friendliness, easy fabrication, and light-to-energy conversion with relatively high efficiency. One of the most important components in the DSSCs is the counter electrode (CE), which collects electrons from external circuit and catalyzes the reduction of triiodide ions in electrolyte. As a conventional CE, Pt is scarce and expensive that makes the cost of DSSCs high and limits the potential large-scale applications. Previous studies have proposed various new materials such as carbon materials, organic polymers or inorganic compounds to replace Pt.[2−6] Compared with carbon materials and organic polymers, inorganic compounds display unique characteristics such as broad variety of materials, good plasticity, and simple preparation.[7] Therefore, making efforts on the preparation of inorganic compounds as substitute of Pt CE may provide a new way to reduce the DSSCs cost. To our knowledge, Lin et al. have synthesized Cu_2ZnSnS_4 (CZTS) by a wet-chemistry approach and fabricated CZTS CE by spin-coated or drop-cast method for DSSCs recently.[8] In their work, CZTS have been demonstrated high electrocatalytic activity as an effective CE material for DSSCs. But stoichiometric CZTSe has not been explored as inorganic CE materials. Because of the similarity of the structure of CZTSe to that of CZTS,[9] and inorganic CZTSe as CE has an advantage for large scale application as being a much more abundant and cheaper feedstock than Pt, with the costs of element for CZTSe several hundred times lower than that of platinum, it can be expected that CZTSe is able to provide Pt-like electrocatalytic properties.

Quaternary chalcogenide CZTSe as photovoltaic materials has attracted much attention owing to its excellent properties such as high absorption coefficients (1×10^5 cm^{-1}),[10] tunable direct band gap (1.0−1.5 eV),[11,12] low toxicity, relative abundance of its elements, and high radiation stability. Various methods have been used for the preparation of CZTSe materials, including physical methods,[13−15] and wet chemical routes.[16−19] However, all of the above reports employed CZTSe materials as absorber layer in thin film cells; there has been no concentration on its application in DSSCs.

One-step solvothermal synthesis of CZTSe does not require either extreme reaction conditions, high fabrication cost, or unique precursors with tedious complicated synthesis procedures. Moreover, solvothermal method to synthesize CZTSe in mild conditions can give a high yield and need not to additional selenization. Thus, stoichiometric CZTSe as CE synthesized by one-step solvothermal method in the solvents of ethylenediamine and water may bring fresh perspective to the scientific research and potential application of DSSCs, in which the solvents need not additional removel.

The CZTSe nanoparticles have been synthesized by one-step solvothermal method,[20,21] but the qualities of CZTSe nanoparticles still need to be improved. Meanwhile, to make element Se dissolve into solution completely at room temperature, we used a small quantity of $N_2H_4{\cdot}H_2O$ to dissolve Se in advance. Furthermore, compared with our previous work,[20] the prepared

Received: January 12, 2012
Accepted: March 2, 2012
Published: March 2, 2012

nanoparticle size in this paper was smaller, bonding to the FTO substrate relatively strong when coating films. As a test to determine if the CZTSe nanoparticles have potential electrocatalytic activity as CE material for DSSCs,[22] we drop-casted CZTSe nanoparticle "inks" of different volumes onto the FTO glass to form different thickness thin films, which were packaged into DSSCs for the first time. The effect of the film thickness on electrocatalytic activity and photovoltaic performance was investigated. The highest solar energy conversion efficiency of 3.85% was achieved. Though the energy conversion efficiency can not reach that of the Pt electrode in our present work, the stoichiometric inorganic compound CZTSe as potential CE shows good catalytic activity for triiodide reduction, and the open-circuit voltages of all DSSCs with CZTSe CE are higher than that of Pt CE.

2. EXPERIMENTAL DETAILS

2.1. Materials. Cupric(II) sulfate anhydrous ($CuSO_4$), zinc(II) nitrate hexahydrate [$Zn(NO_3)_2{\cdot}6H_2O$], tin(IV) chloride pentahydrate ($SnCl_4{\cdot}5H_2O$), selenium powder (Se), anhydrous ethylenediamine, hydrazine hydrate ($N_2H_4{\cdot}H_2O$) and ethanol were all of analytical grade and used without further purification. All water used was obtained from a Millipore Milli-Q purification system.

2.2. Synthesis of CZTSe Nanoparticles. In a typical synthesis, stoichiometric amounts of $CuSO_4$ (0.85 mmol), $Zn(NO_3)_2{\cdot}6H_2O$ (0.43 mmol) and $SnCl_4{\cdot}5H_2O$ (0.43 mmol) were dissolved in 11 mL distilled water under stirring, then anhydrous ethylenediamine (22 mL) was added. After being magnetically stirred for 10 min, the solution was transferred to a 50 mL stainless steel Teflon-lined autoclave, and 3 mL of $N_2H_4{\cdot}H_2O$ dissolving Se (1.7 mmol) was directly put into the autoclave. The autoclave was sealed and maintained at 200 °C for 25 h. After the autoclave was cooled to room temperature naturally, the resulting precipitates were centrifuged and washed several times with distilled water and absolute ethanol to remove any dissoluble byproduct. After being vacuum-dried at 60 °C for 6 h, the final dark product was collected.

2.3. CZTSe Thin Film Deposition and DSSCs Fabrication. Fifty milligrams of CZTSe powder was dispersed in 1 mL of distilled water and sonicated for 10 min to form a uniform nanoparticle "ink". The "ink" was then drop-casted onto the cleaned FTO glass substrate. The drop-casted area was controlled to be 1×1 cm^2 and the thickness of CZTSe was adjusted by the drop volume of "ink" from 50 to 200 μL. The films were fully dried by placing the substrate in a vacuum chamber at room temperature for 24 h and subsequently annealed at 500 °C for 30 min under the protection of argon to obtain CZTSe CE.

The counter Pt electrode was prepared by sputtering Pt of 100 nm on cleaned FTO glass using radio frequency sputtering at power of 150 W and working pressure of 3×10^3 Torr (with argon gas for 60 s). The TiO_2 photoanode with the effective area of 0.6×0.6 cm^2 were fabricated by screen printing technique on FTO conductive glass following the literatures.[23,24] TiO_2 photoanodes were immersed overnight in 0.3 mM ethanolic solution of cis-bis(isothiocyanato)bis(2,2′-bipyridyl-4−4′-dicarboxylato)-ruthenium(II)bis-tetrabutylammonium dye (N-719 as received from Solaronix) at room temperature to absorb the dye. The TiO_2 photoanodes were then taken out and rinsed with ethanol to remove excess dye adsorbed and dried in air at room temperature. The sandwich-type solar cell was assembled by placing the CZTSe CE on the N-719 dye-sensitized photoelectrode (working electrode), and clipped together as an open cell for measurements. The cell was then filled with a liquid electrolyte composed of 0.1 M anhydrous LiI, 0.12 M I_2, 1.0 M 1,2-dimethyl-3-n-propylimidazolium iodide (DMPII), and 0.5 M tert-butylpyridine in dehydrated acetonitrile by capillary force.

2.4. Characterization. The structure of the as-prepared sample were identified by X-ray diffractometer (XRD, Philips X′ Pert Pro Cu−Kα: λ = 0.15406 nm). X-ray photoelectron spectroscopy (XPS) measurements were carried out on an AXIS ULTRA spectrometer using Al Kα X-ray as the excitation source. The morphology was characterized by field emission scanning electron microscopy (FESEM, JEOL JSM-7001F) and transmission electron microscopy (TEM, JSM-2010), respectively. Element analysis of the product was measured by energy-dispersive spectrometer (EDS) equipped with the above FESEM. The Raman spectrum was recorded using a LABRAM-1B confocal laser micro-Raman spectrometer with the wavelength of 632.8 nm. Cyclic voltammetry (CV) was carried out in a three-electrode system in an acetonitrile solution of 0.1 M $LiClO_4$, 10 mM LiI, and 1 mM I_2 at a scan rate of 50 mVs^{-1}. Platinum served as a counter electrode and the Ag/Ag+ couple was used as a reference electrode. The photocurrent−voltage (J−V) measurements were taken on a digital source meter (Keithley 2400, computer-controlled) with the device under AM 1.5 G spectrum, which was produced by a solar simulator (Newport, Oriel class A, SP91160A, USA). The light power density was calibrated against a Si-based reference cell (Hamamatsu S1133) to accurately simulate the full-sun intensity (100 mW cm^{-2}).

3. RESULTS AND DISCUSSION

Figure 1a shows the corresponding XRD pattern of the prepared CZTSe nanoparticles. The major XRD diffraction peaks appeared at 2θ = 27.14, 45.12, 53.45, 65.86, 72.48, and 83.48° can be attributed to (112), (204), (312), (400)/(008), (316),

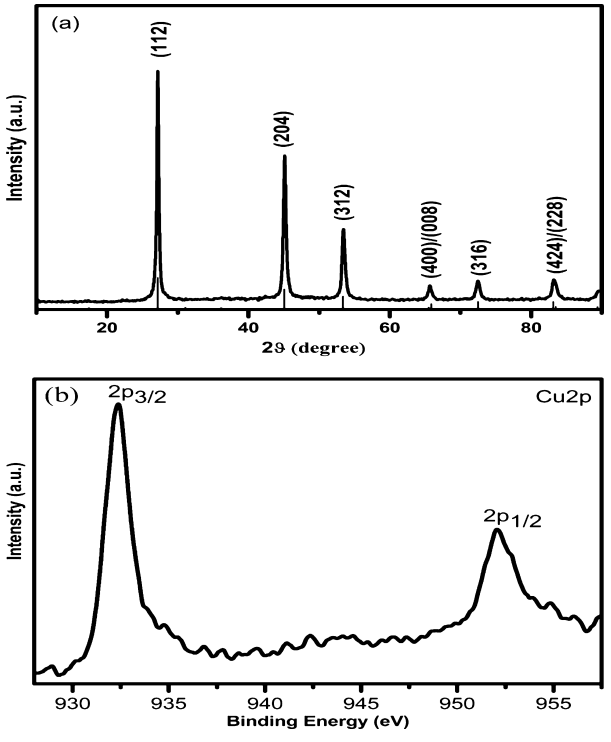

Figure 1. (a) Powder XRD pattern of the nanoparticles and (b) XPS spectrum of the constituent element: copper 2p.

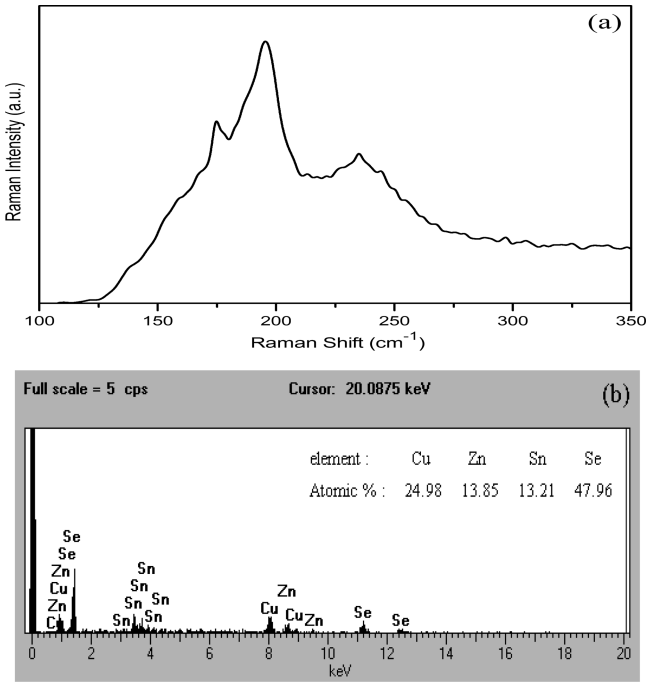

Figure 2. (a) Raman scattering analysis and (b) elemental composition of CZTSe nanoparticles measured by EDS.

and (424/228) planes, respectively. All the diffraction peaks are compatible with those of tetragonal CZTSe (JCPDS Card, No. 52−0868). On the basis of the XRD pattern, the lattice parameters (a and c) calculated from the *d*-spacing of Jade 5 software were found to be a = 0.569 nm and c = 1.133 nm, which were close to the data reported by other reports.[25,26]

The diffraction peaks of stoichiometric Cu_2SnSe_4 and ZnSe are very similar to those of CZTSe. It is insufficient to determine the phase purity of the CZTSe from XRD pattern alone.[27] To role out the impurity phases, XPS analysis was used to confirm the expected oxidation states of all four elements in the CZTSe nanoparticles.The Cu 2p, Zn 2p, Sn 3d, and Se 3d core levels were examined, respectively. Strong peaks of Cu $2p_{3/2}$ and Cu $2p_{1/2}$ located at 932.4 and 952.2 eV with a peak splitting of 19.8 eV (Figure 1b) are well-consistent with the reported values for Cu^+.[28] Moreover, no satellite peak of Cu^{2+} at about 942 eV for Cu_2SnSe_4[29,30] is observed in the present XPS spectrum. Hence, it is well proved that there is no existence of Cu_2SnSe_4 phase. The Zn 2p peaks located at 1022.1 and 1045.0 eV in Figure S1a (see the Supporting Information) show a peak separation of 22.9 eV, consistent with the standard splitting of 22.97 eV, suggesting Zn^{2+}. In the spectrum of Sn 3d (see Figure S1b in the Supporting Information), it is observed that two peaks locate at 486.6 and 495.1 eV corresponding to Sn $3d_{5/2}$ and Sn $3d_{3/2}$, indicating of Sn^{4+} with a peak splitting of 8.5 eV. The binding energy of Se $3d_{5/2}$ peak in the spectrum (see Figure S1c in the Supporting Information) is 54.1 eV, which is in good agreement with the literature values for Se^{2-}.[29,31−34]

For ZnSe, the characteristic peaks of ZnSe are positioned at 252 and 205 cm^{-1} in Raman spectrum,[35−37] but there is no evidence of ZnSe peak in the Raman analysis (Figure 2a), confirming no ZnSe phase in the product. On the contrary, the three main peaks of CZTSe are observed at 196, 175, and 234 cm^{-1}, suggesting the chemical composition of the sample is CZTSe.[21,35,38]

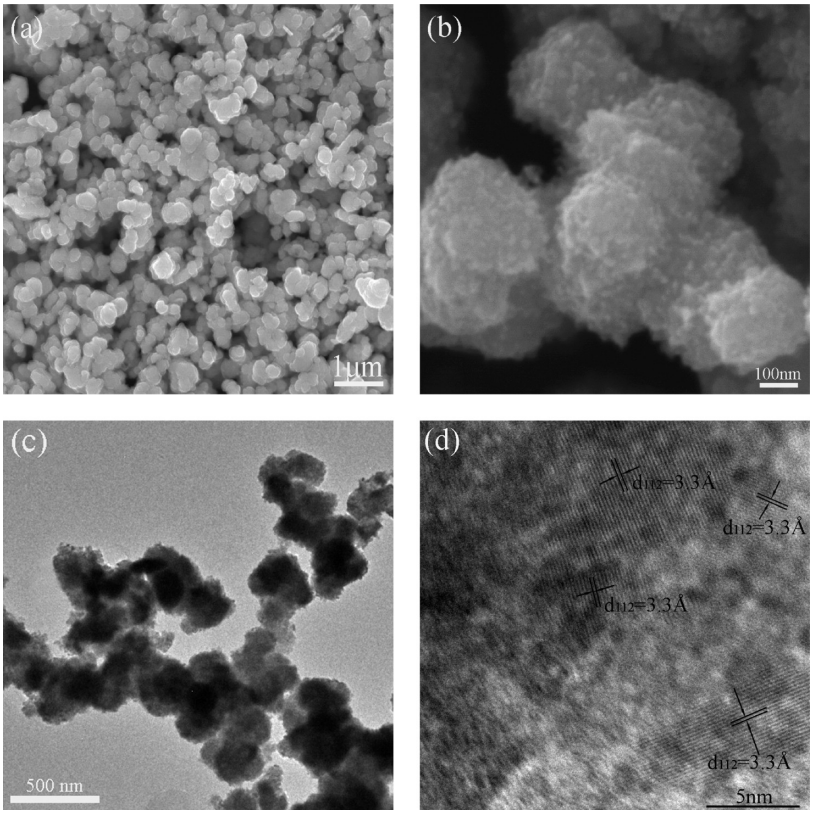

Figure 3. FESEM images of the as-obtained CZTSe nanoparticles with (a) low and (b) high magnifications, (c) TEM image and (d) HRTEM image of the as-obtained CZTSe nanoparticles.

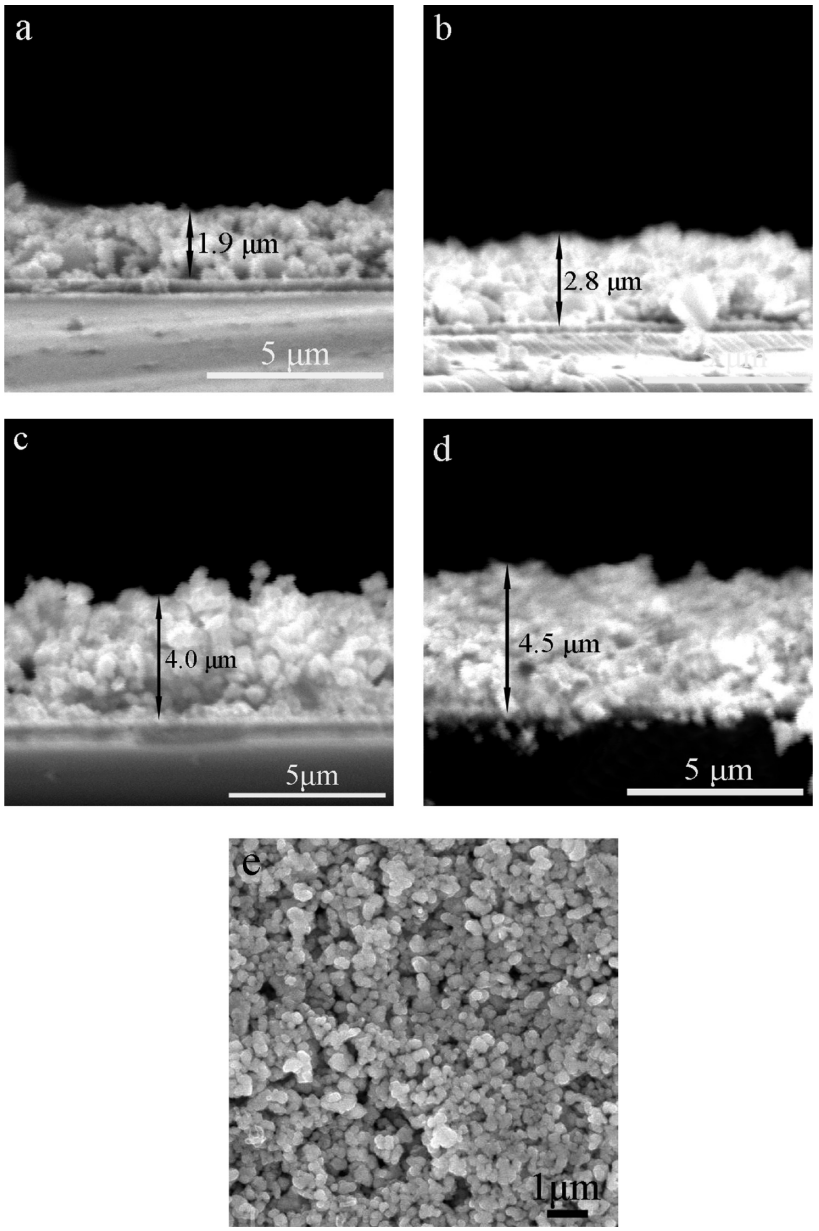

Figure 4. (a–d) cross-sectional FESEM images of CZTSe thin film with drop volume of (a) 50, (b) 100, (c) 150, and (d) 200 μL. (e) Corresponding top view FESEM image of CZTSe thin film with 100 μL drop volume.

The EDS spectrum confirmed the sample was exactly composed of Cu, Zn, Sn and Se elements (Figure 2b). Taking the Se element as the reference, the atom ratio of Cu, Zn, Sn, Se is determined to be 2.08:1.15:1.10:4.00. Considering the error of the EDS detector (approximately ±2 atom %), this value is almost stoichiometric. On the basis of the above analysis, we can conclude that the sample is pure stoichiometric CZTSe.

The morphology of as-synthesized CZTSe nanoparticles was demonstrated by FESEM and TEM images. As shown in Figure 3a, the nanoparticles are relatively uniform and the average nanoparticle sizes are in the range of 200–300 nm. Figure 3b is a high-magnification FESEM micrograph of CZTSe nanoparticles, it can be seen that the nanoparticle surfaces are considerably rough. Based on the calculation by Debye–Scherrer formula from XRD result, the nanoparticles are composed of numerous tiny nanocrystals with an average crystallite size of 21.5 nm. Some of the tiny nanocrystals can be seen from the edge of some nanoparticles in Figure 3c. Nearly spherical nanoparticles connected with each other are randomly distributed in Figure 3c, the diameters of the nanoparticles are about 200–300 nm, which are in accordance with the FESEM results. The lattice fringe of 3.3 Å (Figure 3d) matches the spacing distance of (112) plane and agrees well with that determined from the diffraction peak at 27.14° in XRD pattern,[39,40] moreover, the nanocrystals with different growth directions in Figure 3d indicate many nanocrystals in individual nanoparticle.

To ensure the effect of anneal on the CZTSe composition, we characterized XRD, XPS, and EDS measurements of CZTSe powders annealed in the same condition. As shown in Figure S2 in the Supporting Information, all the diffraction peaks can be indexed to CZTSe. The observed values of the binding energies for Cu $2p_{3/2}$ and Cu$2p_{1/2}$ with a interval of 19.8 eV in the XPS spectrum (see Figure S3 in the Supporting Information) of Cu 2p are in agreement with the literatue

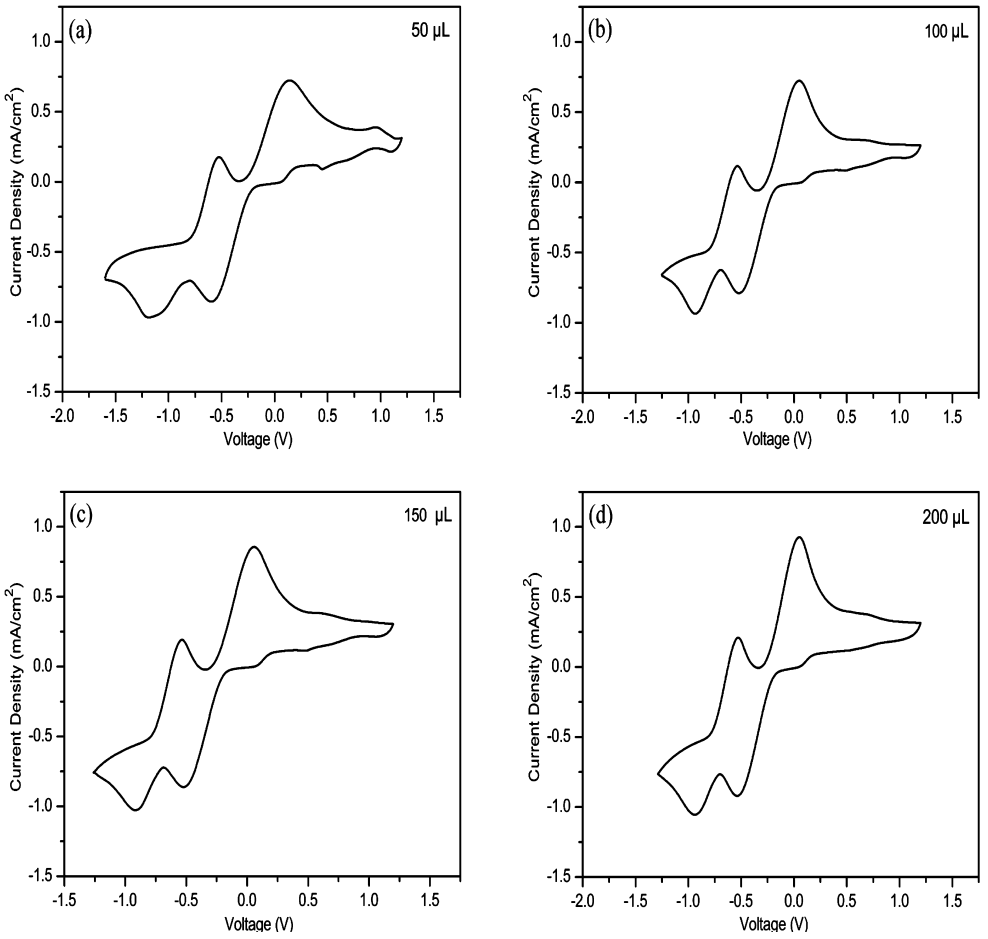

Figure 5. Cyclic voltammograms (CVs) of CZTSe counter electrodes with different thickness. The electrolyte solution was composed of 0.1 M $LiClO_4$, 10 mM LiI, and 1 mM I_2 in acetonitrile. The scan rate was 50 mV/s. Pt electrode was used as CE and Ag/Ag+ works as reference electrode.

values,[28,29] suggesting only Cu^+ exits in this compound. EDS measurement was carried out to determine the compositions (see Figure S4 in the Supporting Information). The atom ratio is Cu:Zn:Sn:Se = 1.96:0.90:1.06:4.00, that is close to the theoretical value of 2:1:1:4. The above results demonstrate that annealing cannot effect the composition of CZTSe.

The cross-sectional FESEM images of the CZTSe thin film after anneal are presented in Figure 4a-d, increasing the drop volume gives rise to an increase in film thickness, from 1.9 to 4.5 μm. Figure 4e shows the top view FESEM image of CZTSe thin film with the drop volume of 100 μL of after heat treatment. It can be seen that after heat treatment, the nanoparticle morphology and size are the same as those of without anneal (see Figure 3a).

Cyclic voltammetry (CV) experiments were carried out to characterize the electrocatalytic activity of CZTSe CE under I^-/I_3^- electrochemical system using three-electrode system. As shown in Figure 5, the cyclic voltammograms of I^-/I_3^- redox reaction on different CZTSe CE are similar, two pairs of redox peaks are observed. The left pair of peaks are corresponding to the redox reaction 1 (eq 1), whereas the right ones are corresponding to the reaction 2 (eq 2).[41] When the drop volume is 50 μL, the cathodic peak position assigned to the redox reaction 1 is slightly negative (Figure 5a), indicating a relatively stronger catalysis than the others.[7] The current density increases gradually with increasing the film thickness, which can be attributed to more electrocatalytic sites in thicker films. It can be seen that the CZTSe CE exhibits Pt-like performance in DSSCs.

$$I_3^- + 2e^- \rightleftharpoons 3I^- \quad (1)$$

$$3I_2 + 2e^- \rightleftharpoons 2I_3^- \quad (2)$$

Figure 6 shows the $J-V$ curves of N-719 DSSCs with different thickness CZTSe CEs and Pt CE. The corresponding

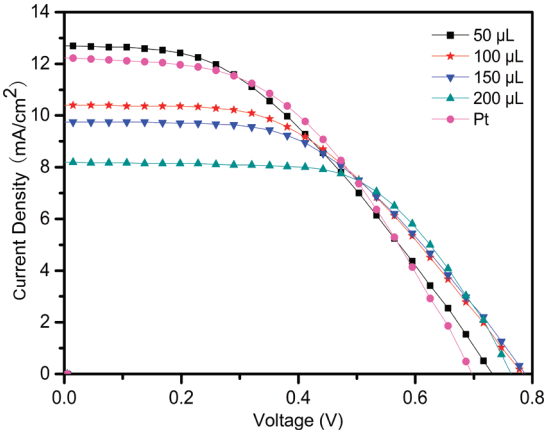

Figure 6. $J-V$ characteristics of DSSCs with different thickness CZTSe CEs and Pt CE.

photovoltaic parameters are summarized in Table1. When the drop volume was 100 μL, the thickness of CZTSe film was

dx.doi.org/10.1021/am3000616 | ACS Appl. Mater. Interfaces 2012, 4, 1796–1802

Table 1. Photovoltaic Performance of DSSCs with Different Thickness CZTSe CEs and Pt CE[a]

samples	thickness (μm)	J_{sc} (mA/cm^2)	V_{oc} (V)	FF (%)	efficiency (η%)
50 μL	1.9	12.69	0.73	41.19	3.82
100 μL	2.8	10.39	0.78	47.31	3.85
150 μL	4.0	9.76	0.79	49.50	3.80
200 μL	4.5	8.18	0.76	60.49	3.78
Pt	0.1	12.23	0.70	47.27	4.03

[a] J_{sc}, short-circuit current density; V_{oc}, open-circuit voltage; FF: fill factor.

approximately 2.8 μm (Figure 4b), and a highest efficiency of η = 3.85% was achieved with J_{sc} = 10.39 mA/cm^2, V_{oc} = 0.78 V, and FF = 47.31%. When the drop volume was 200 μL, the photovoltaic parameters J_{sc} (8.18 mA/cm^2) and V_{oc} (0.76 V) were little lower, resulting in a relatively poor efficiency η (3.78%). From Table 1, it can be seen clearly that the photocurrent density decreases significantly with increasing drop volume, from 12.69 to 8.18 mA/cm^2. That is to say, thicker film is not beneficial to the charges transport. The decline of J_{sc} may be attributed to high resistance for charge transport because of a thicker film being used,[7] whereas the fill factor increases from 41.19% to 60.49% with the increase of the film thickness. Unlike Pt electrode, the prepared film is composed of small nanoparticles and porous (Figure 4e). With the increase in the film thickness, CZTSe CE provides relatively larger amount of electrocatalytic sites that is beneficial to the electrocatalytic activity and leads to the increase of the fill factor. Meanwhile, a higher resistance is caused by more abundant grain boundaries and defects in thicker film, which reduces the electrical conductivity and thus the photocurrent density.[7,42] Because of the improvement in FF and the reduction in J_{sc}, the power conversion efficiency changes unconspicuously when adjusting the film thickenss.[43,44] Compared with the Pt electrode, though the energy conversion efficiency is little lower than that of the Pt electrode in our present work, all the V_{oc} values of CZTSe CE, and the fill factors of CZTSe CE with drop volumes greater than 50 μL, are higher than those of Pt CE. Metal selenide can be used in DSSCs as demonstrated in this work.

4. CONCLUSIONS

In summary, this work presents a simple and convenient synthesis of relatively uniform CZTSe nanoparticles. In the reaction system, common inorganic metal salts and element Se were used as reactants, ethylenediamine and water were used as the solvents. The structure, composition and morphology of the as-obtained nanoparticles were characterized by various methods. DSSCs with CZTSe thin film as low-cost CE candidate were fabricated. The CV result demonstrated the Pt-like electrocatalytic activity of the synthesized CZTSe film. The photovoltaic properties of the DSSCs were also investigated. A highest solar energy conversion efficiency of 3.85% was achieved. Photovoltaic measurement showed that the thickness of the film affected the photocurrent density and fill factor remarkably. Further work will be focused on the improvement of the energy conversion efficiency by optimizing the parameters, such as the film density, the film thickness, assembly technology of solar cells, and so on.

■ ASSOCIATED CONTENT

Supporting Information

XPS analysis for Zn 2p, Sn 3d, and Se 3d before anneal. XRD, XPS for Cu 2p, and EDS of CZTSe powder annealed at 500 °C. The resistivities of the CZTSe thin films prepared on glass substrate as a function of the film thickness. This material is available free of charge via the Internet at http://pubs.acs.org.

■ AUTHOR INFORMATION

Corresponding Author

*E-mail: wusixin@henu.edu.cn., Tel./fax: +86 378 3881358.

Notes

The authors declare no competing financial interest.

■ ACKNOWLEDGMENTS

This project is supported by the National Natural Science Foundation of China (20871041 and 20903033), the New Century Excellent Talents in University (NCET-08-0659), and the Scientific Research Foundation of Henan University (SBGJ090510 and 2010YBZR014).

■ REFERENCES

(1) Ahmad, S.; Yum, J. H.; Butt, H. J.; Nazeeruddin, M. K.; Gratzel, M. *Chem. Phys. Chem.* **2010**, *11*, 2814−2819.
(2) Trancik, J. E.; Barton, S. C.; Hone, J. *Nano Lett.* **2008**, *8*, 982−987.
(3) Xia, J.; Masaki, N.; Jiang, K.; Yanagida, S. *J. Mater. Chem.* **2007**, *17*, 2845−2850.
(4) Wang, M. K.; Anghel, A. M.; Marsan, B.; Ha, N. C.; Pootrakulchote, N.; Zakeeruddin, S. M.; Gratzel, M. *J. Am. Chem. Soc.* **2009**, *131*, 15976−15977.
(5) Xia, J. B.; Yuan, C. C.; Yanagida, S. *ACS Appl. Mater. Interfaces* **2010**, *2*, 2136−2139.
(6) Li, G. R.; Song, J.; Pan, G. L.; Gao, X. P. *Energy Environ. Sci.* **2011**, *4*, 1680−1683.
(7) Wu, M. X.; Lin, X.; Hagfeldt, A.; Ma, T. L. *Angew. Chem.* **2011**, *123*, 3582−3586.
(8) Xin, X. K.; He, M.; Han, W.; Jung, J.; Lin, Z. Q. *Angew. Chem.* **2011**, *123*, 11943−11946.
(9) Chen, S.; Walsh, A.; Yang, J. H.; Gong, X. G.; Sun, L.; Yang, P. X.; Chu, J. H.; Wei, S. H. *Phys. Rev. B* **2011**, *83*, 125201.
(10) Shavel, A.; Arbiol, J.; Cabot, A. *J. Am. Chem. Soc.* **2010**, *132*, 4514−4515.
(11) Chen, S. Y.; Gong, X. G.; Walsh, A.; Wei, S. H. *Appl. Phys. Lett.* **2009**, *94*, 041903.
(12) Shi, L.; Pei, C. J.; Li, Q.; Xu, Y. M. *J. Am. Chem. Soc.* **2011**, *133*, 10328−10331.
(13) Wibowo, R. A.; Lee, E. S.; Munir, B.; Kim, K. H. *Phys. Stat. Sol. A* **2007**, *204*, 3373−3379.
(14) Salome, P. M. P.; Fernandes, P. A.; da Cunha, A. F.; Leit, J. P.; Malaquias, J.; Weber, A.; et al. *Sol. Energy Mater. Sol. Cells* **2010**, *94*, 2176−2180.
(15) Volobujeva, O.; Raudoja, J.; Mellikov, E.; Grossberg, M.; Bereznev, S.; Traksmaa, R. *J. Phys. Chem. Solids* **2009**, *70*, 567−570.
(16) Todorov, T. K.; Reuter, K. B.; Mitzi, D. B. *Adv. Mater.* **2010**, *22*, E156−E159.
(17) Liu, W. L.; Wu, M. Q.; Yan, L. D.; Zhou, R. C.; Si, S. X.; Zhang, S. R.; Zhang, Q. Y. *Mater. Lett.* **2011**, *65*, 2554−2557.
(18) Haas, W.; Rath, T.; Pein, A.; Rattenberger, J.; Trimmel, G.; Hofer, F. *Chem. Commun.* **2011**, *47*, 2050−2052.
(19) Barkhouse, D. A. R.; Gunawan, O.; Gokmen, T.; Todorov, T. K.; Mitzi, D. B. *Prog. Photovolt.: Res. Appl.* **2012**, *20*, 6−11.
(20) Du, Y. F.; Zhou, W. H.; Zhou, Y. L.; Li, P. W.; Fan, J. Q.; He, J. J.; Wu, S. X. *Mater. Sci. Semicond. Process.* **2011**, DOI: 10.1016/j.mssp.2011.09.005.
(21) Cao, Y.; Wang, C. R.; Hu, J. Q. *Adv. Mater. Res.* **2011**, *347*−*353*, 848−851.
(22) Steinhagen, C.; Akhavan, V. A.; Goodfellow, B. W.; Panthani, M. G.; Harris, J. T.; Holmberg, V. C.; Korgel, B. A. *ACS Appl. Mater. Interfaces* **2011**, *3*, 1781−1785.

(23) Zhang, Q. X.; Guo, X. Z.; Huang, X. M.; Huang, S. Q.; Li, D. M.; Luo, Y. H.; Shen, Q.; Toyoda, T.; Meng, Q. B. *Phys. Chem. Chem. Phys.* **2011**, *13*, 4659−4667.
(24) Li, D. M.; Wang, M. Y.; Wu, J. F.; Zhang, Q. X.; Luo, Y. H.; Yu, Z. X.; Meng, Q. B.; Wu, Z. J. *Langmuir* **2009**, *25*, 4808−4814.
(25) Matsushuta, H.; Maeda, T.; Katsui, A.; Takazawa, T. *J. Cryst. Growth* **2000**, *208*, 416−422.
(26) Schorr, S.; Weber, A.; Honkimäki, V.; Schock, H. W. *Thin Solid Films* **2009**, *517*, 2461−2464.
(27) Guo, Q. J.; Ford, G. M.; Yang, W. C.; Walker, B. C.; Stach, E. A.; Hillhouse, H. W.; Agrawal, R. *J. Am. Chem. Soc.* **2010**, *132*, 17384−17386.
(28) Riha, S. C.; Parkinson, B. A.; Prieto, A. L. *J. Am. Chem. Soc.* **2009**, *131*, 12054−12055.
(29) Li, B.; Xie, Y.; Huang, J. X.; Qian, Y. T. *Adv. Mater.* **1999**, *11*, 1456−1459.
(30) Chen, X. Y.; Wang, X.; An, C. H.; Liu, J. W.; Qian, Y. T. *J. Cryst. Growth* **2003**, *256*, 368−376.
(31) Chen, H. Y.; Yu, S. M.; Shin, D. W.; Yoo, J. B. *Nanoscale Res. Lett.* **2010**, *5*, 217−223.
(32) Bindu, K.; Sudha Kartha, C.; Vijayakumar, K. P.; Abe, T.; Kashiwaba, Y. *Sol. Energy Mater. Sol. Cells* **2003**, *79*, 67−79.
(33) Danilson, M.; Altosaar, M.; Kauk, M.; Katerski, A.; Krustok, J.; Raudoja, J. *Thin Solid Films* **2011**, *519*, 7407−7411.
(34) Wang, J. J.; Wang, Y. Q.; Cao, F. F.; Guo, Y. G.; Wan, L. J. *J. Am. Chem. Soc.* **2010**, *132*, 12218−12221.
(35) Salome, P. M. P.; Fernandes, P. A.; da Cunha, A. F. *Thin Solid Films* **2009**, *517*, 2531−2534.
(36) Lu, G. W.; An, H. Z.; Chen, Y.; Huang, J. H.; Zhang, H. Z.; Xiang, B.; Zhao, Q.; Yu, D. P.; Du, W. M. *J. Cryst. Growth* **2005**, *274*, 530−535.
(37) Venkatachalam, S.; Agilan, S.; Mangalaraj, D.; Narayandass, Sa. K. *Mater. Sci. Semicond. Process.* **2007**, *10*, 128−132.
(38) Grossberg, M.; Krustok, J.; Timmo, K.; Altosaar, M. *Thin Solid Films* **2009**, 2489−2492.
(39) Han, S. K.; Kong, M. G.; Guo, Y.; Wang, M. T. *Mater. Lett.* **2009**, *63*, 1192−1194.
(40) Zou, C.; Zhang, L. J.; Lin, D. S.; Yang, Y.; Li, Q.; Xu, X. J.; Chen, X. A.; Huang, S. M. *Cryst. Eng. Comm.* **2011**, *13*, 3310−3313.
(41) Sun, H. C.; Qin, D.; Huang, S. Q.; Guo, X. Z.; Li, D. M.; Luo, Y. H.; Meng, Q. B. *Energy Environ. Sci.* **2011**, *4*, 2630−2637.
(42) Li, G. R.; Wang, F.; Jiang, Q. W.; Gao, X. P.; Shen, P. W. *Angew. Chem.* **2010**, *122*, 3735−3738.
(43) Xu, F.; Sun, L. T.; Dai, M.; Lu, Y. N. *J. Phys. Chem. C* **2010**, *114*, 15377−15382.
(44) Qiu, J. H.; Guo, M.; Wang, X. D. *ACS Appl. Mater. Interfaces* **2011**, *3*, 2358−2367.